Copy No. 129

RM No. L8H25a

NACA

RESEARCH MEMORANDUM

STATIC TESTS OF FOUR TWO-BLADE NACA PROPELLERS DIFFERING IN CAMBER AND SOLIDITY

By

Robert J. Platt, Jr.

Langley Aeronautical Laboratory
Langley Field, Va.

NATIONAL ADVISORY COMMITTEE
FOR AERONAUTICS

WASHINGTON

December 2, 1948

Supersedes PT-15 (5)

NACA RM No. L8H25a

NATIONAL ADVISORY COMMITTEE FOR AERONAUTICS

RESEARCH MEMORANDUM

STATIC TESTS OF FOUR TWO-BLADE NACA PROPELLERS DIFFERING IN CAMBER AND SOLIDITY

By Robert J. Platt, Jr.

SUMMARY

Outdoor static tests were made on two-blade propellers of the NACA 4-(3)(08)-03, 4-(5)(08)-03, 4-(10)(08)-03, and 4-(3)(08)-045 designs. The blade angles tested ranged from 0° to 40° measured at the 0.75R station. The maximum tip Mach number was 0.93, but this value was not attained at blade angles above 15° because flutter was encountered. However, some data on the NACA 4-(5)(08)-03 and 4-(10)(08)-03 propellers operating in the flutter region are included which were obtained in an earlier static test (unpublished).

The results of the test of the high-camber blade, NACA 4-(10)(08)-03, indicated the thrust coefficient reached a maximum and began to decrease at a tip Mach number of about 0.85 for fixed blade angle settings of 15° and less. Similar breaks did not occur for the blades of lower camber up to the maximum tip Mach number attained. The maximum value of the ratio of thrust coefficient to power coefficient C_T/C_P, which occurred at low power coefficients, decreased with increasing camber, blade width, and tip Mach number. Except in the region of maximum C_T/C_P, the ratio C_T/C_P increased with both increasing camber and blade width for a constant value of power coefficient. At the higher power coefficients the value of C_T/C_P for a given value of power coefficient was but little affected by tip Mach number.

INTRODUCTION

The effects of compressibility, camber, and blade width on the characteristics of two-blade propellers were investigated by the National Advisory Committee for Aeronautics in the Langley 8-foot high-speed tunnel and have been presented in a series of papers (references 1 to 3). The propellers incorporated high-critical-speed NACA 16-series airfoil sections with thin sections used at the shank. The operating characteristics of the Langley 8-foot high-speed tunnel did not permit the measurements to be made at low speeds and, consequently, data at low advance ratios could not be obtained. This made impractical the extrapolation of the data to zero advance ratio to obtain static-test data.

Propeller data at static conditions are useful for take-off run calculations and propeller selection. The effect of tip speed, airfoil section, and blade width on static propeller characteristics has been previously investigated (reference 4). However, the blades used were conventional with round shank sections and were designed for operation at low advance ratios. The results, then, could not be expected to apply directly to the propellers used in an investigation at the Langley 8-foot high-speed tunnel. In order to obtain the characteristics of these latter propellers at static conditions, a propeller dynamometer, located outdoors, was used to measure the thrust and torque of the propellers over a range of tip Mach number and blade angle.

SYMBOLS

b	blade width, feet
C_P	power coefficient $\left(\frac{P}{\rho n^3 D^5}\right)$
C_T	thrust coefficient $\left(\frac{T}{\rho n^2 D^4}\right)$
c_{l_d}	design section lift coefficient
D	propeller diameter, feet
h	blade-section maximum thickness, feet
M_t	tip Mach number
n	propeller rotational speed, revolutions per second
P	power, foot-pound per second
R	propeller tip radius, feet
r	radius to a blade element, feet
T	thrust, pounds
β	blade angle, degrees
ρ	air density, slugs per cubic foot

APPARATUS

The propeller dynamometer consists of two independent units similar to the unit shown in figure 1. One unit is located ahead of the propeller and the other behind the propeller. Each unit contains two 200-horsepower induction motors, but only the rear unit was connected to the propeller for this investigation.

Some details of the rear dynamometer may be seen from figure 1. The two motors are coupled and mounted within a shell to make the motors a single rigid unit. This motor assembly is floated within the outer dynamometer barrel by air bearings. Compressed air is supplied to these bearings which are located at each end of the motor shell. The motor assembly is then free to move within the outer barrel in an axial direction under thrust and to rotate under torque. This movement is restrained by hydraulic thrust and torque capsules mounted at the rear of the dynamometer. In this system air bearings are again employed to prevent interaction of the thrust and torque forces. The hydraulic lines are connected to compensating scales for the measurement of thrust and torque. The dynamometer is supported from an overhead framework by a streamline strut through which pass the motor electrical and cooling water leads.

The blades were of the NACA 4-(3)(08)-03, 4-(5)(08)-03, 4-(10)(08)-03, and 4-(3)(08)-045 designs, and are identical with those used in the tests of references 1 to 3. The number designations of these blades are descriptive of their size and shape. The number of the first group gives the propeller diameter in feet. The numbers within the first parentheses represent the design lift coefficient (in tenths) at the 0.7R station. The numbers within the second parentheses represent the thickness ratio (in hundredths) of the blade section at 0.7R. The last group of numbers represents the solidity (in hundredths or thousandths, for two and three digits, respectively) of one blade at 0.7R.

The blades incorporated the NACA 16-series airfoil sections and were designed for minimum induced-energy loss at a blade angle of approximately 45° measured at the 0.7R station. The NACA 4-(3)(08)-03 and 4-(3)(08)-045 blades are shown in figure 2. The other blades are similar to the NACA 4-(3)(08)-03, except for the higher blade-section design lift coefficients. The blade-form curves for these propellers are shown in figures 3 and 4.

A cylindrical spinner of a 13-inch diameter (the diameter of the front and rear dynamometer outer casings) was used with the propellers. Therefore, only efficient airfoil sections were exposed to the air. Each propeller consisted of two blades constructed of aluminum alloy.

TESTS

The blade angles at which the propellers were tested ranged from 0° to 40° (measured at 0.75R) in 5° increments. The construction of the spinner did not permit the propellers to be tested at negative blade angles. Thrust, torque, and rotational speed of the propeller were measured at intervals of 500 revolutions per minute. Two readings were taken at each rotational speed and a few were repeated as the rotational speed was decreased after reaching the maximum speed.

For reasons of safety, the maximum rotational speed was limited to 5000 revolutions per minute; but even this speed was not attained at blade angles above 15° because flutter was encountered. An estimate of the rotational speed at which flutter began, as shown in figure 5 in terms of tip Mach number, was made by visual and aural means. Additional data at speeds up to 5000 revolutions per minute, obtained from earlier static tests of the NACA 4-(5)(08)-03 and 4-(10)(08)-03 propellers operating in the flutter region, are, however, included herein.

The data were reduced to the usual thrust and power coefficients C_T and C_P. The tip Mach number M_t was based on the rotational tip speed of the propeller. Typical data obtained are shown in figure 6. Where only one point is shown at a test rotational speed, the readings were identical.

Figure 7 presents typical data from the earlier static test in which operation of the propellers was extended into the flutter region. The internal mechanism of the dynamometer used in this earlier test was different from that of the present dynamometer, although the dynamometers were outwardly similar. Repeat runs showed poor agreement and differences in the faired curves of as much as 15 percent were found at the higher blade angles. These discrepancies may have been due to the friction which was definitely present in this earlier dynamometer and to different section maximum lift coefficients caused by varying roughness of the blades. No spinner was used in this earlier test.

The results of both the earlier and the present investigations include the effects of blade twist under aerodynamic and centrifugal forces. This twist was not measured, but the results of reference 5 indicate that its magnitude at the 0.7R station was of the order of 0.2° to 0.3° at the highest rotational speed and was in the direction of increasing blade angle.

RESULTS AND DISCUSSION

The basic data for the four two-blade propellers used in this investigation are shown in figures 8 to 15. The dashed curves in figures 10 to 13 are from the earlier investigation and, in most cases,

were obtained with the propeller fluttering at the higher tip Mach numbers. Although the accuracy of these earlier data is questionable, it is presented here because little high-tip Mach number data were obtained in the present investigation at the higher blade angles. In cases where repeat runs were made for a given blade angle, the run which showed closest agreement with data from the present investigation was chosen for presentation in figures 10 to 13.

Considering the dashed curves in figures 10 to 13, large increases in the coefficients are found with increasing tip speed in some cases. These increases begin with the onset of flutter. In the cases of the NACA 4-(5)(08)-03 propeller at $\beta_{0.75R} = 35^\circ$ and the NACA 4-(10)(08)-03 propeller at $\beta_{0.75R} = 20^\circ$, no flutter was encountered in this earlier investigation and no sudden increase in the coefficients was found. It appears then that the marked rise in the value of the thrust and power coefficients with increasing rotational speed is caused, at least in part, by the flutter itself. Since the accuracy of these earlier data is poor, the following discussion will be concerned only with the data obtained in the present investigation.

At the low blade angles, increasing tip speed produces a gradual increase in thrust and power coefficients (figs. 8 to 15). The effect of tip speed is most pronounced on the high-camber blade, NACA 4-(10)(08)-03 (fig. 12), in that the thrust coefficient reaches a maximum and begins to decrease at a tip Mach number of about 0.85. Since the critical speed of the highly cambered sections is relatively low, this earlier compressibility loss is to be expected and is in accord with the results of wind-tunnel tests (references 3 and 6) in which it was found that the high-camber blade suffered efficiency losses at a tip Mach number well below that of the lower-camber blades.

At the high blade angles, there is generally a decrease in the coefficients with tip Mach number for all the propellers, particularly in the thrust coefficient.

The thrust and power coefficients for the four propellers tested have been plotted against blade angle for a constant tip Mach number of 0.45 in figures 16 and 17. The thrust-coefficient curves are similar to the lift curves of airfoils, and an increase in design lift coefficient would be expected, as the data indicate, to increase the thrust coefficient at a given blade angle. However, the difference in thrust coefficient between the NACA 4-(3)(08)-03 and the 4-(5)(08)-03 propellers is not great. Figure 17 indicates that there is also little difference in the power coefficients of these two propellers. Comparison of the NACA 4-(3)(08)-03 propeller with the wider-blade NACA 4-(3)(08)-045 propeller indicates that increasing blade width has the effect of increasing the slope of the thrust-coefficient curve and is accompanied by an increase in the power coefficient over the blade-angle range tested.

The ratio of thrust coefficient to power coefficient is usually used as a static-thrust figure of merit for propellers operating at the same

tip speed. This ratio is plotted in figure 18 against blade angle for the four propellers at a tip Mach number of 0.45. The decrease in the maximum value of C_T/C_P with increasing camber is probably the result of increasing induced velocities and, in the case of the highly cambered blade, lower lift-drag ratios. At medium blade angles, however, C_T/C_P increases with camber. This may be explained partially by the fact that the angle of attack for the maximum lift-drag ratio increases with camber for the NACA 16-series airfoils, which effectively shifts the C_T/C_P-curves of the higher-camber blades to higher blade angles. The effect of widening the blades, holding a fixed value of camber, is to decrease the maximum value of C_T/C_P with but little change in C_T/C_P at the higher blade angles.

A more useful comparison of the propellers can be made by plotting C_T/C_P against C_P as shown in figure 19. For a given power coefficient, the curves show an improvement in the static thrust coefficient with increasing camber, especially from increasing the design lift coefficient from 0.5 to 1.0, and with increasing blade width. Higher values of C_T/C_P are produced by the higher-camber and wider-blade propellers, since, for the same power coefficient, the angles of attack along the blade are lower and less stalling results.

The effect of tip speed on the ratio of thrust coefficient to power coefficient is shown in figure 20 for blade angles of 5°, 10°, and 15°. In general, C_T/C_P decreases with tip speed for a given blade-angle setting and the decrease is more pronounced as the camber is increased. For a given power coefficient, C_T/C_P does not necessarily decrease with tip speed as shown in figure 21 where C_T/C_P is plotted against C_P for both a high and a low tip Mach number. At the higher power coefficients there is, in fact, an increase in C_T/C_P for the narrow blades when the tip Mach number is increased from 0.45 to 0.90. The maximum value of C_T/C_P does, however, decrease with tip Mach number.

CONCLUSIONS

Static tests of four two-blade NACA propellers to a maximum tip Mach number of 0.93 indicated the following conclusions:

1. The results of the test of the high-camber blade, NACA 4-(10)(08)-03, indicated the thrust coefficient reached a maximum and began to decrease at a tip Mach number of about 0.85 for fixed blade-angle settings of 15° and less. Similar breaks did not occur for the blades of lower camber up to the maximum tip Mach number attained.

2. The maximum value of the ratio of thrust coefficient to power coefficient C_T/C_P, which occurred at low power coefficients, decreased with increasing camber, blade width, and tip Mach number.

3. Except in the region of maximum C_T/C_P, the ratio C_T/C_P increased with both increasing camber and blade width for a constant value of power coefficient. At moderate values of power coefficient, the greatest thrust was produced by the propeller of the highest camber. At the higher values of power coefficient (above 0.04 per blade), the greatest thrust was produced by the wider-blade propeller.

4. At the higher power coefficients, the value of C_T/C_P for a given value of power coefficient was but little affected by tip Mach number.

Langly Aeronautical Laboratory
National Advisory Committee for Aeronautics
Langley Field, Va.

REFERENCES

1. Stack, John, Draley, Eugene C., Delano, James B., and Feldman, Lewis: Investigation of Two-Blade Propellers at High Forward Speeds in the NACA 8-Foot High-Speed Tunnel. I - Effects of Compressibility. NACA 4-308-03 Blade. NACA ACR No. 4A10, 1944.

2. Stack, John, Draley, Eugene C., Delano, James B., and Feldman, Lewis: Investigation of Two-Blade Propellers at High Forward Speeds in the NACA 8-Foot High-Speed Tunnel. II - Effects of Compressibility and Solidity. NACA 4-308-045 Blade. NACA ACR No. 4B16, 1944.

3. Delano, James B.: Investigation of Two-Blade Propellers at High Forward Speeds in the NACA 8-Foot High-Speed Tunnel. III - Effects of Camber and Compressibility. NACA 4-(5)(08)-03 and NACA 4-(10)(08)-03 Blades. NACA ACR No. L5F15, 1945.

4. Hartman, Edwin P., and Biermann, David: Static Thrust and Power Characteristics of Six Full-Scale Propellers. NACA Rep. No. 684, 1940.

5. Hartman, Edwin P., and Biermann, David: The Torsional and Bending Deflection of Full-Scale Aluminum-Alloy Propeller Blades under Normal Operating Conditions. NACA Rep. No. 644, 1938.

6. Maynard, Julian D., and Salters, Leland B., Jr.: Aerodynamic Characteristics at High Speeds of Related Full-Scale Propellers Having Different Blade-Section Cambers. NACA RM No. L8E06, 1948.

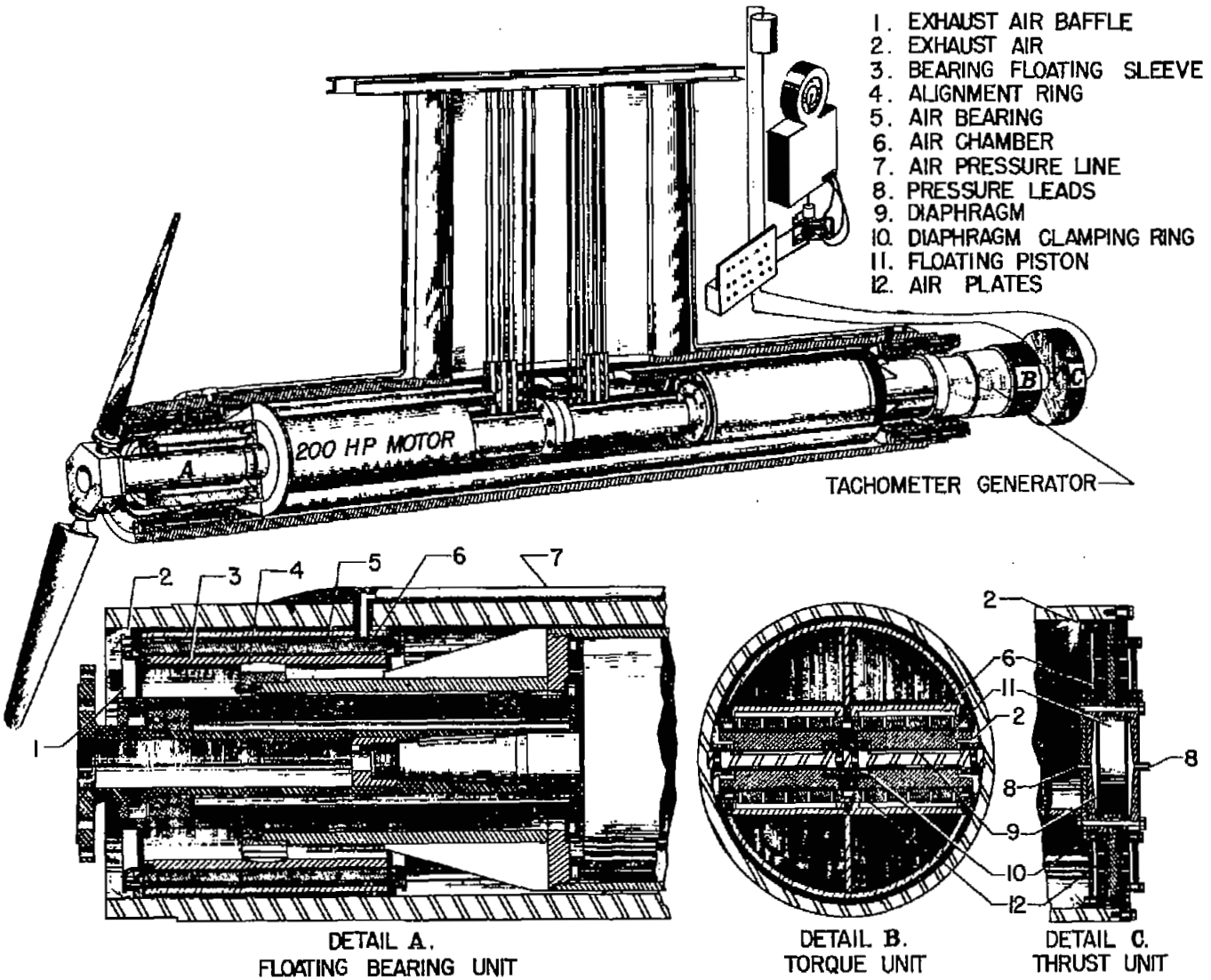

Figure 1.- Cutaway view of one unit of the 800-horsepower dynamometer.

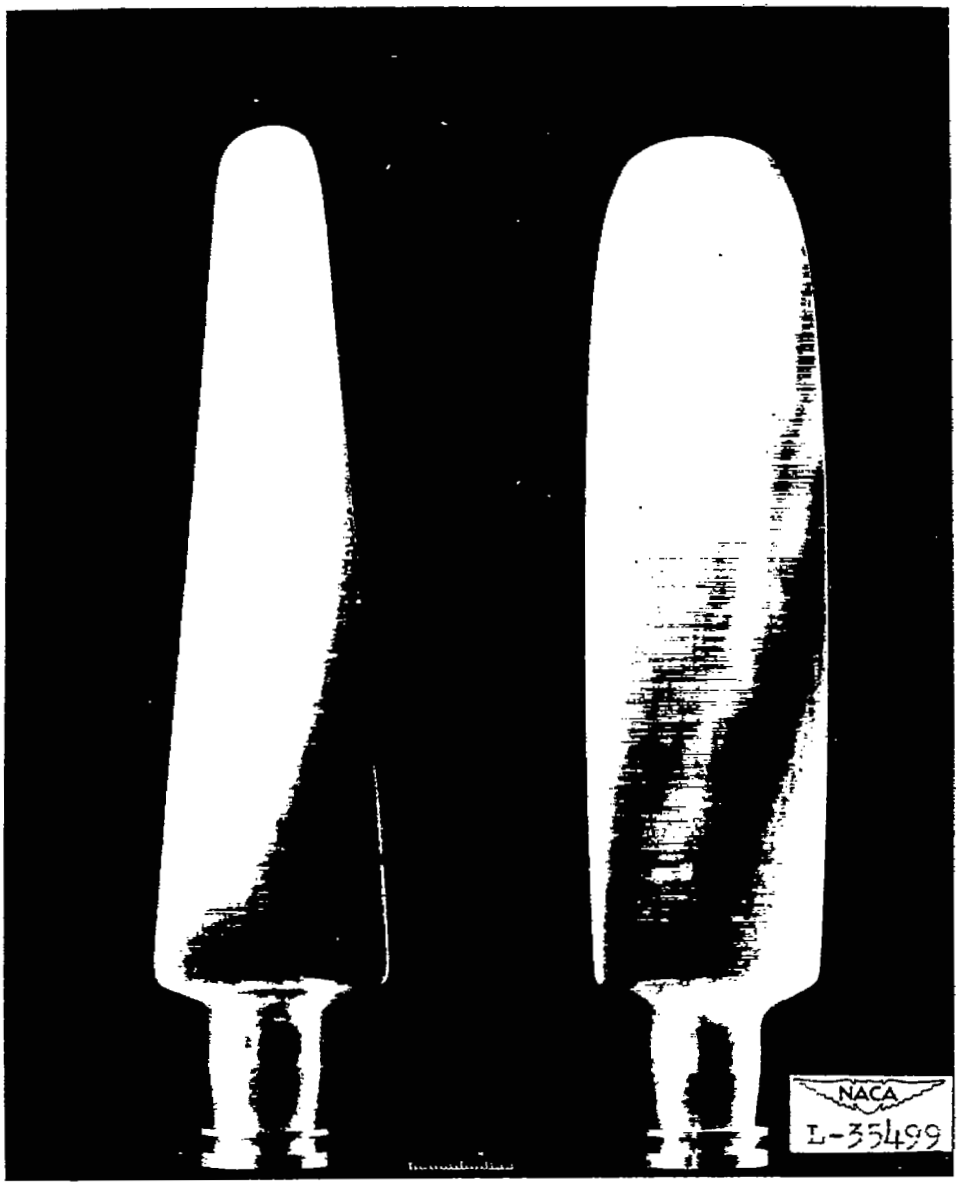

(a) NACA 4-(3)(08)-03. (b) NACA 4-(3)(08)-045.

Figure 2.- Solidity family of NACA 16-series propellers tested.

NACA
L-35499

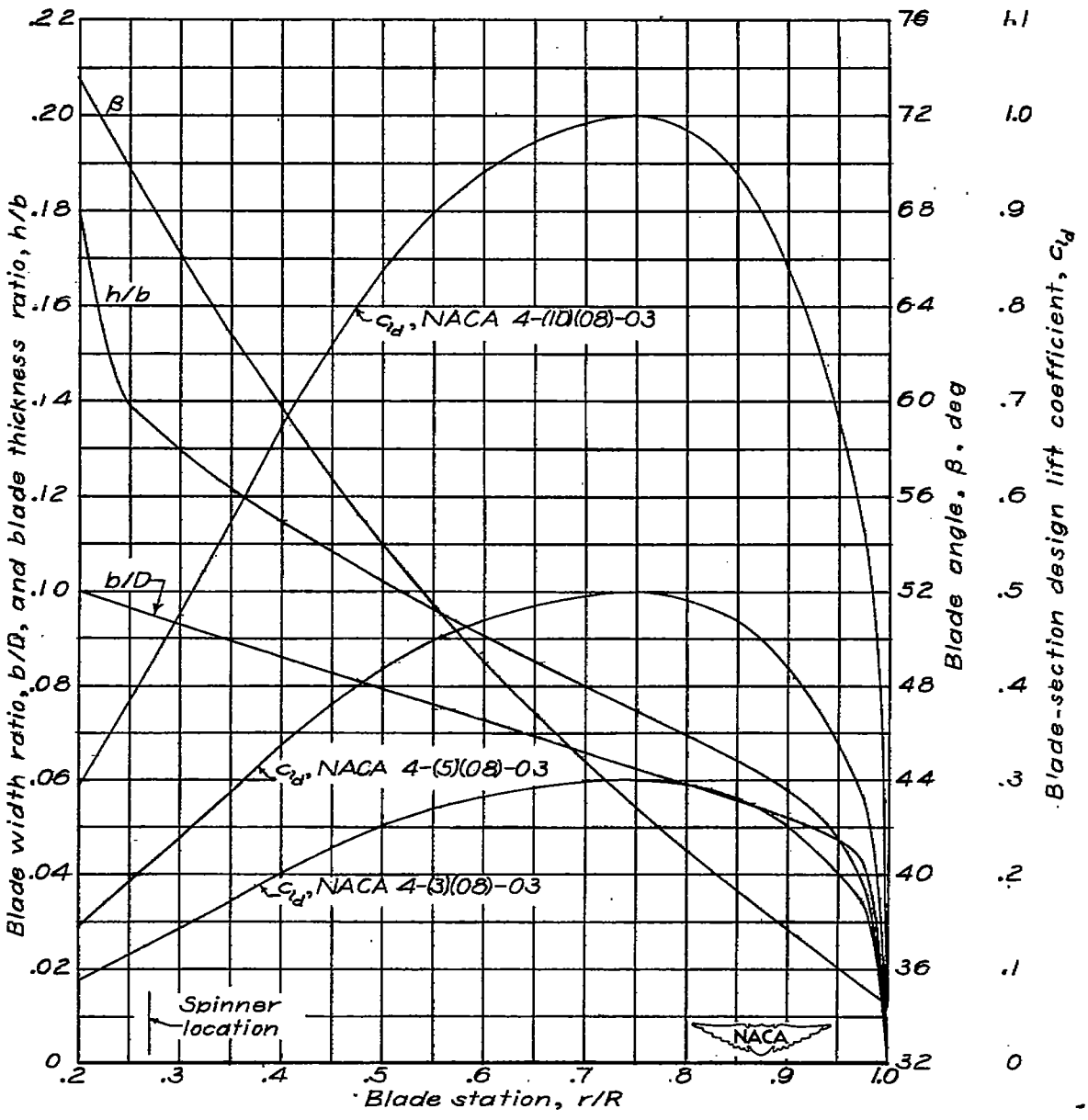

Figure 3.- Blade-form curves for the camber-series two-blade NACA propellers.

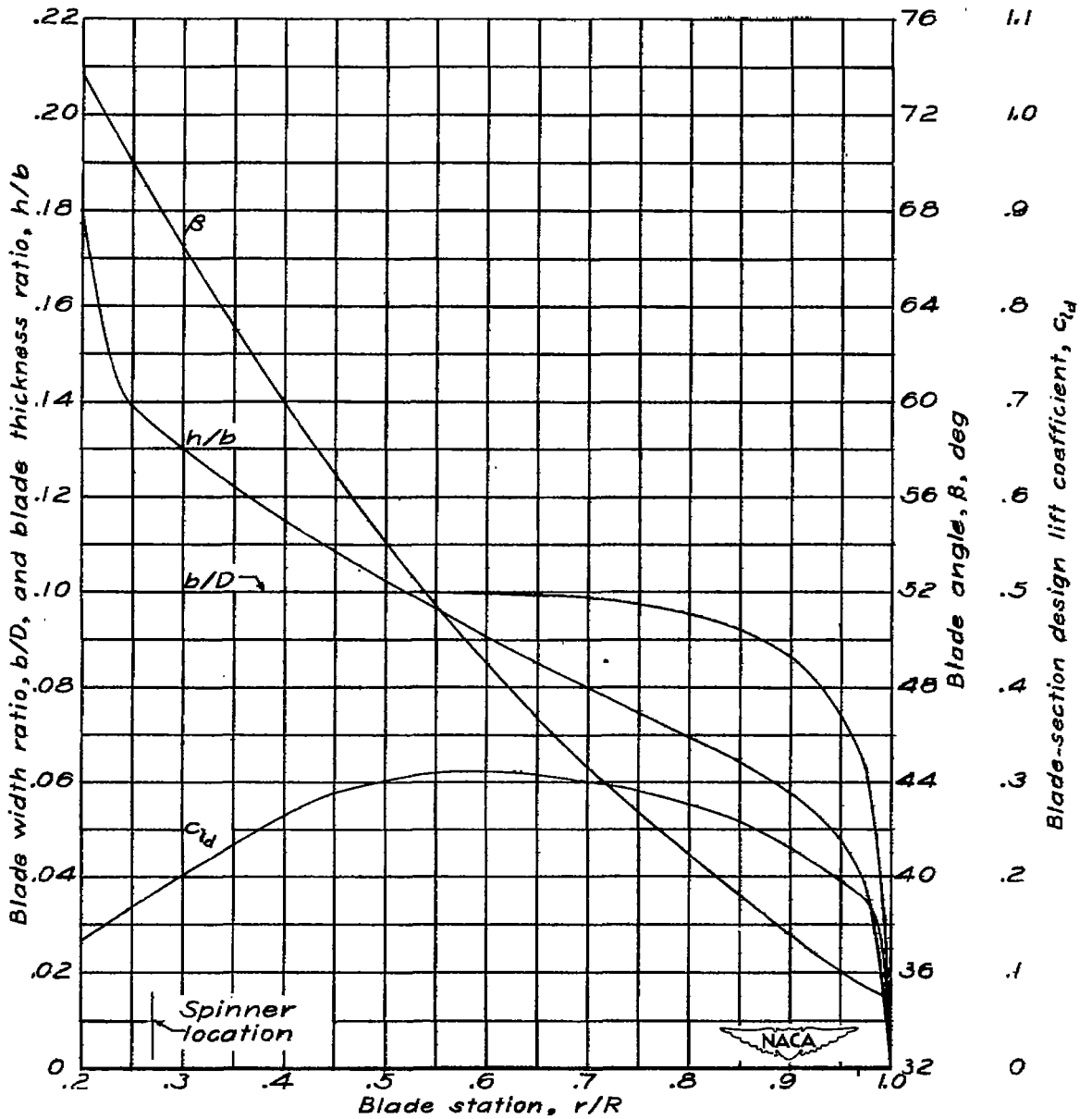

Figure 4.- Blade-form curves for the NACA 4-(3)(08)-045 propeller.

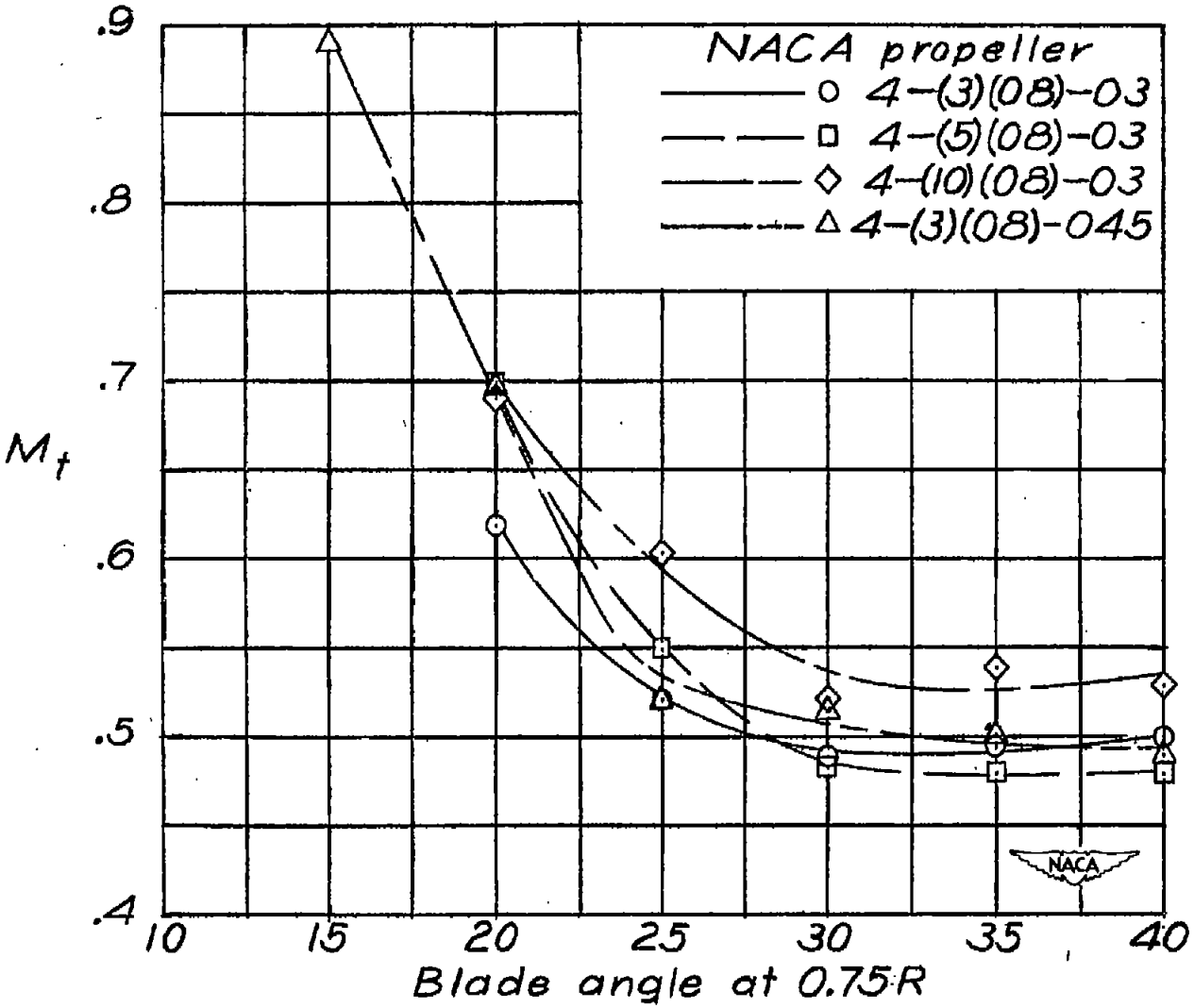

Figure 5.- Approximate variation of flutter speed with blade angle for the two-blade NACA propellers.

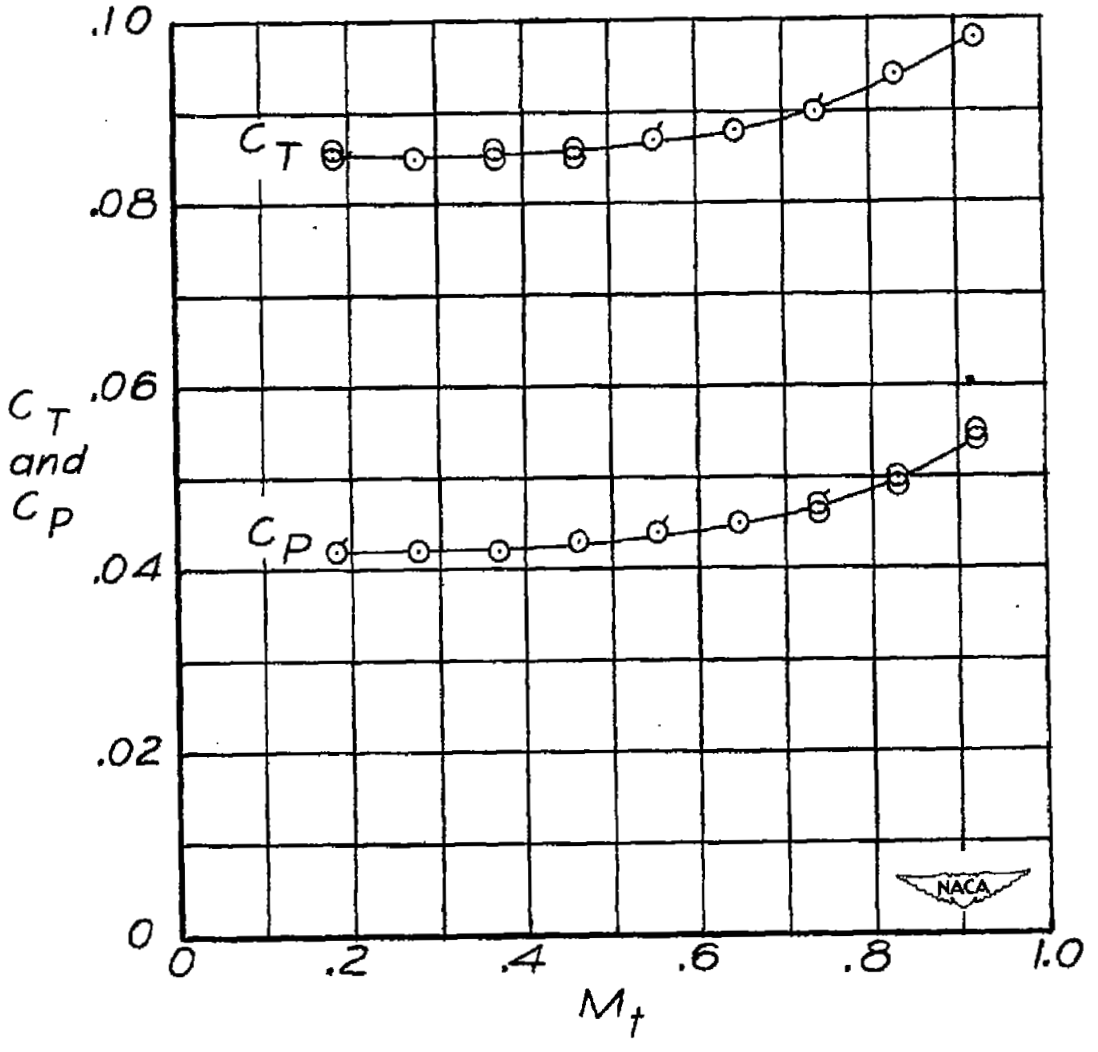

Figure 6.- Typical test results. NACA 4-(3)(08)-03 propeller; two blades; $\beta_{0.75R} = 15^{\circ}$. Flagged symbols indicate data taken with the rotational speed decreasing.

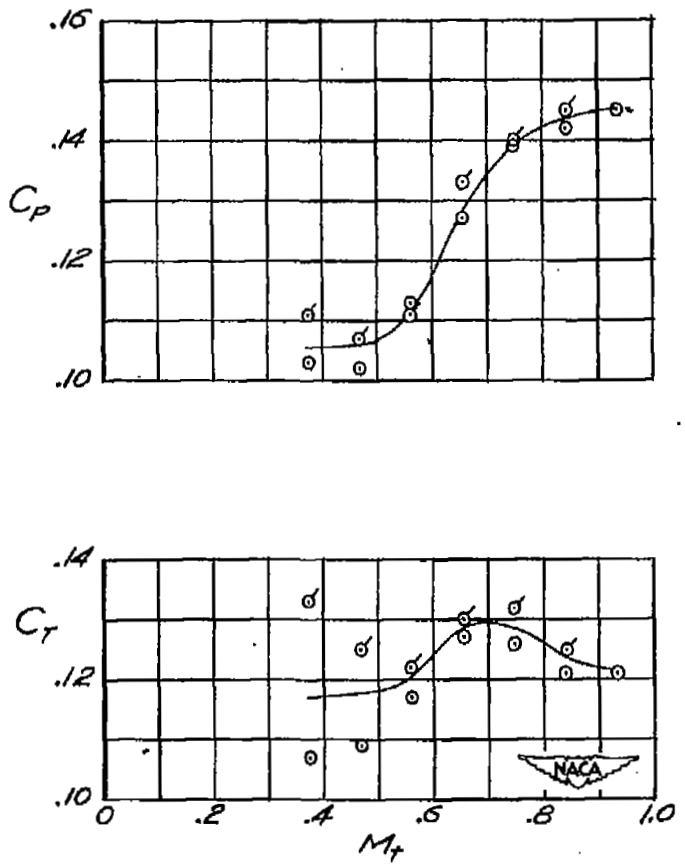

Figure 7.- Typical earlier test results. NACA 4-(5)(08)-03 propeller; two blades; $\beta_{0.75R} = 25^{\circ}$. Flagged symbols indicate data taken with the rotational speed decreasing.

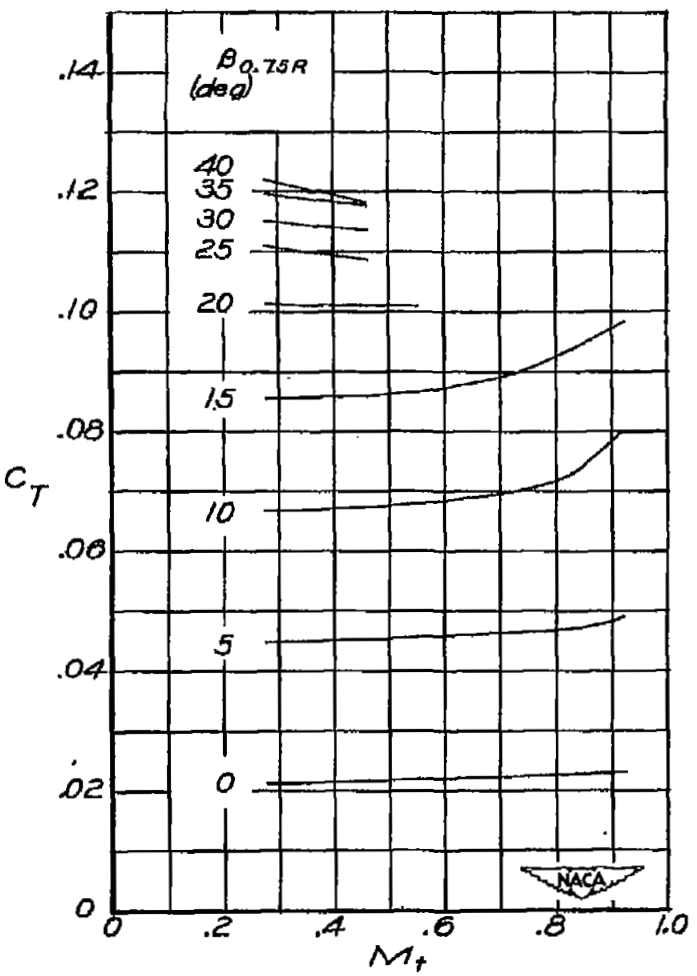

Figure 8.- Variation of static thrust coefficient with tip Mach number. NACA 4-(3)(08)-03 propeller; two blades.

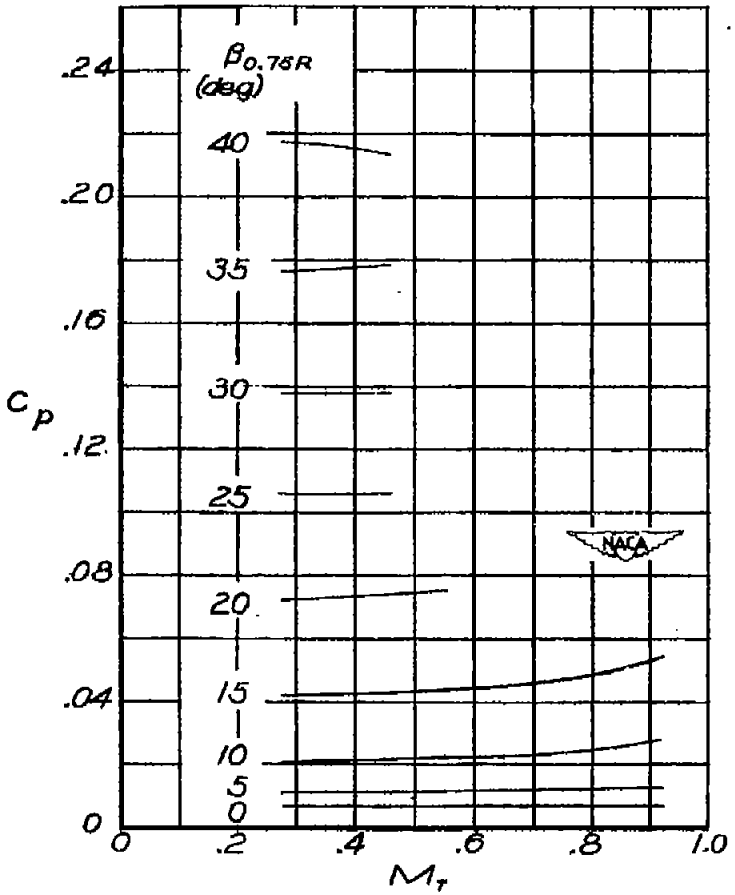

Figure 9.- Variation of static power coefficient with tip Mach number. NACA 4-(3)(08)-03 propeller; two blades.

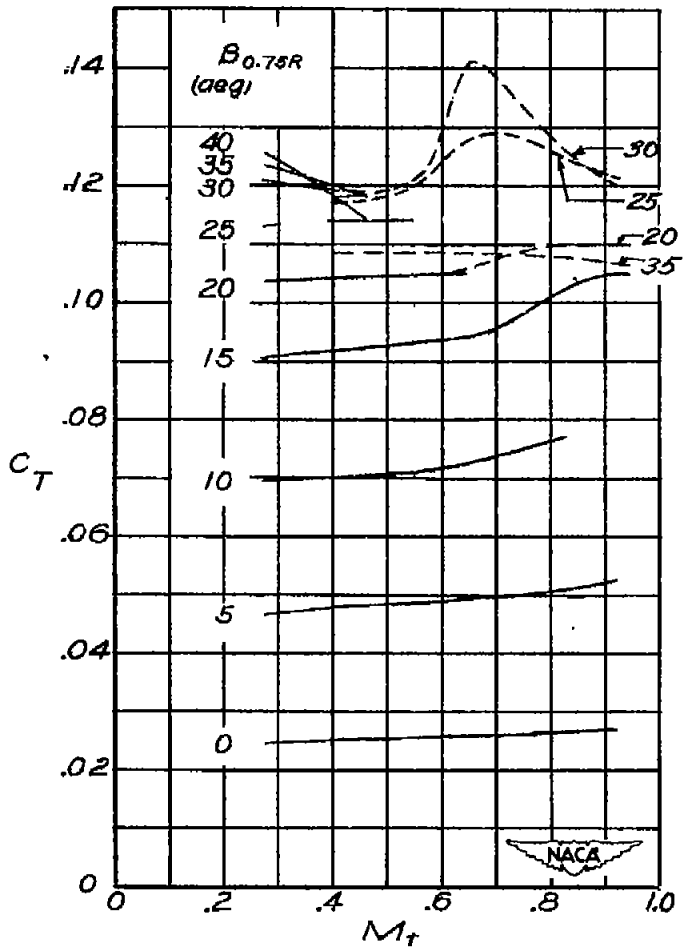

Figure 10.- Variation of static thrust coefficient with tip Mach number. NACA 4-(5)(08)-03 propeller; two blades. Dashed curves are from earlier test.

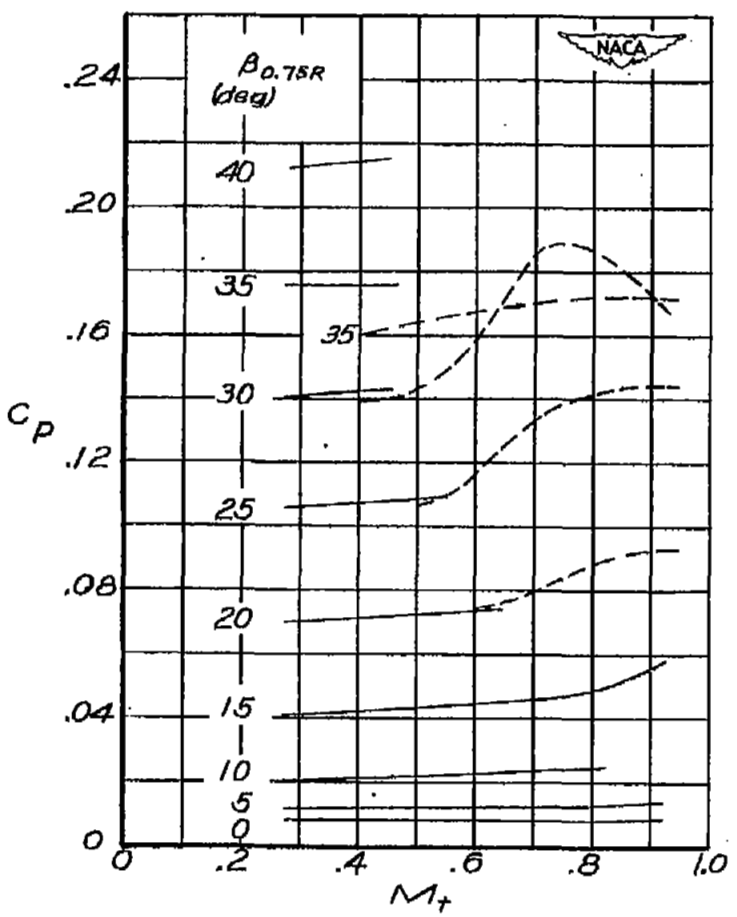

Figure 11.- Variation of static power coefficient with tip Mach number. NACA 4-(5)(08)-03 propeller; two blades. Dashed curves are from earlier test.

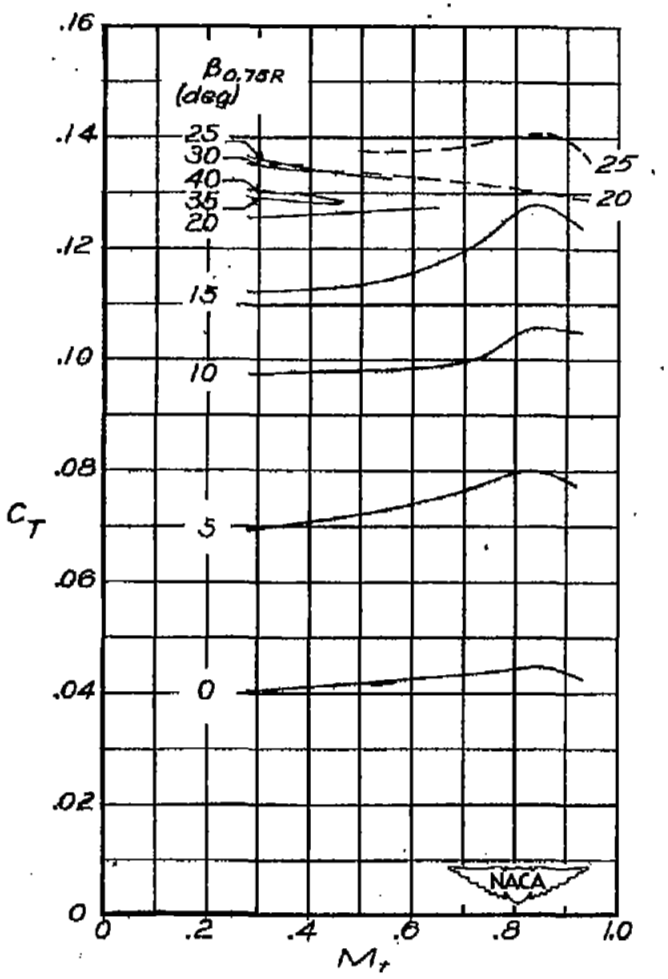

Figure 12.- Variation of static thrust coefficient with tip Mach number. NACA 4-(10)(08)-03 propeller; two blades. Dashed curves are from earlier test.

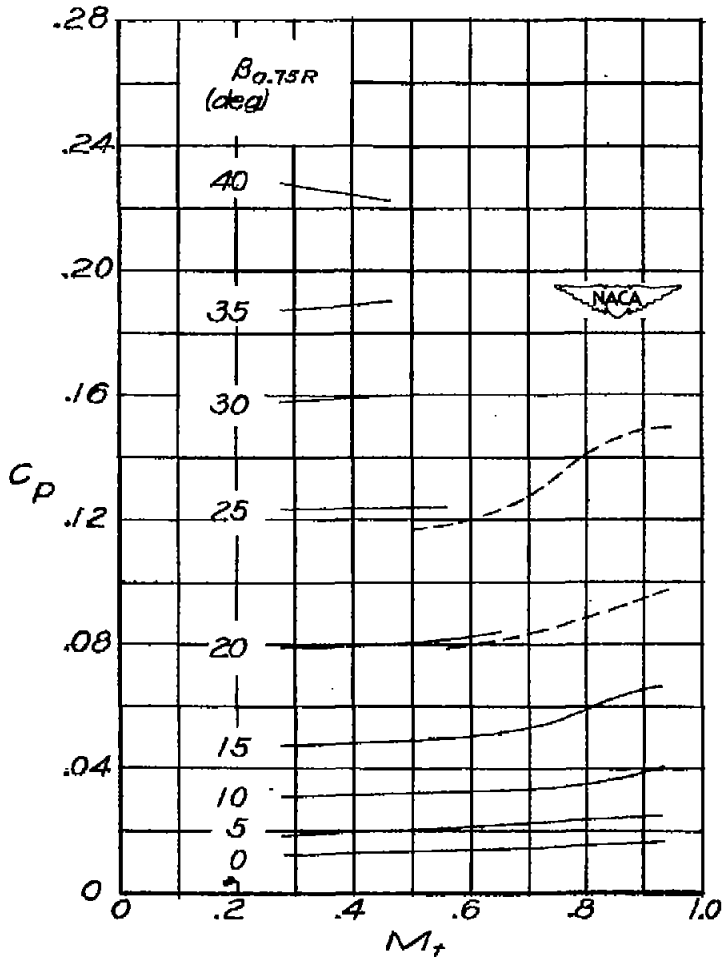

Figure 13.- Variation of static power coefficient with tip Mach number. NACA 4-(10)(08)-03 propeller; two blades. Dashed curves are from earlier test.

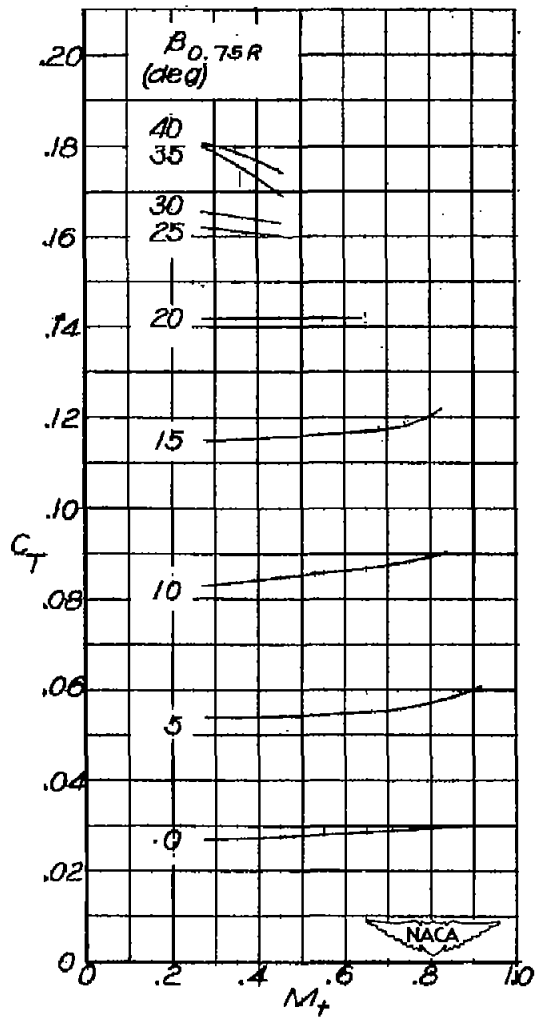

Figure 14.- Variation of static thrust coefficient with tip Mach number. NACA 4-(3)(08)-045 propeller; two blades.

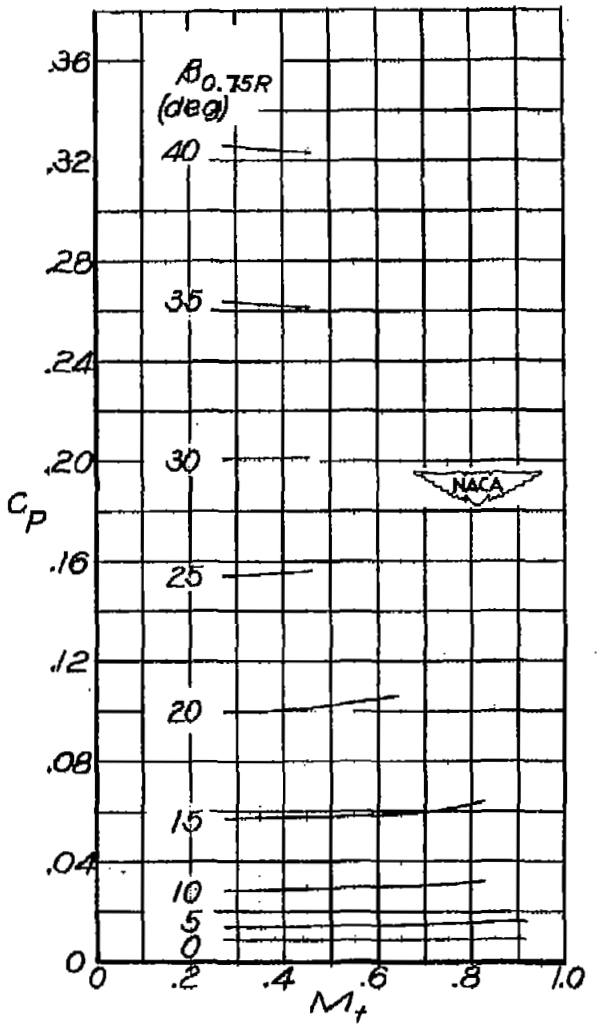

Figure 15.- Variation of static power coefficient with tip Mach number. NACA 4-(3)(08)-045 propeller; two blades.

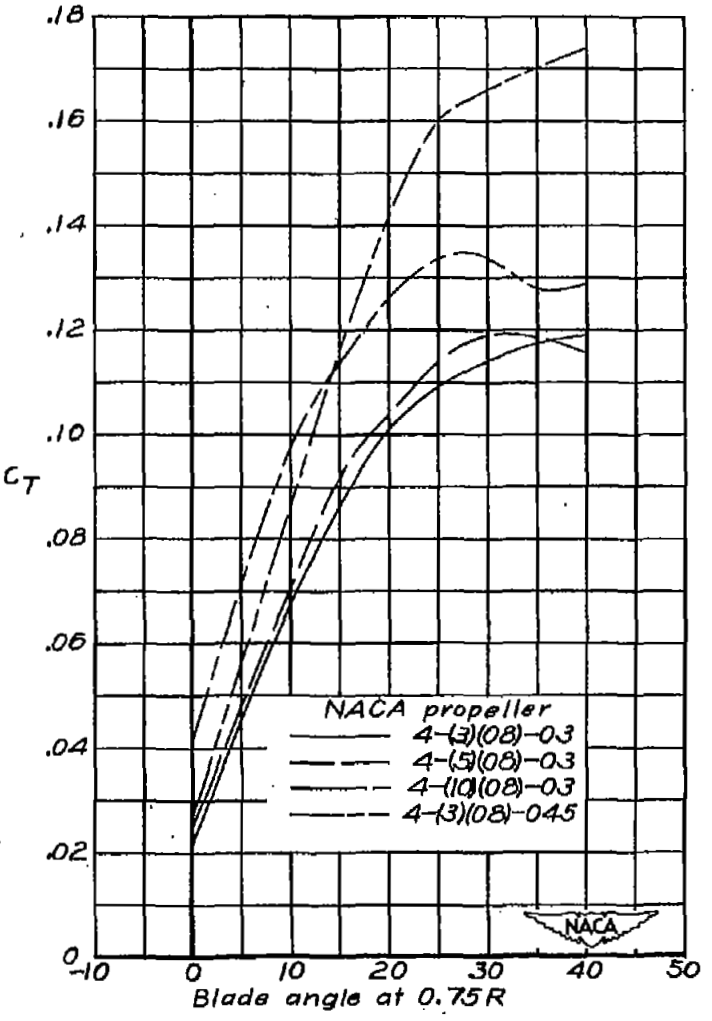

Figure 16.- Comparison of static thrust characteristics of the two-blade NACA propellers. M_t = 0.45.

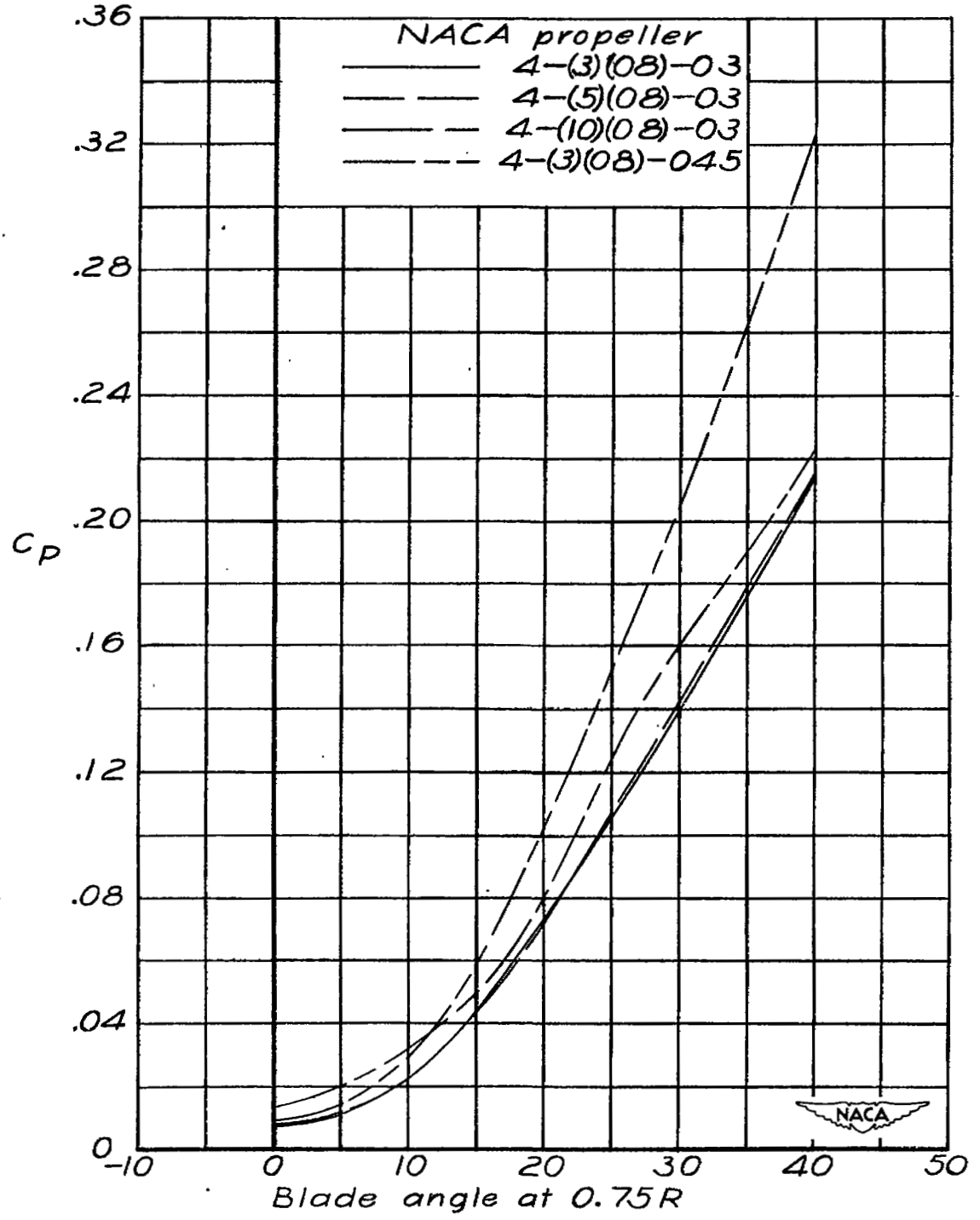

Figure 17.- Comparison of static power characteristics of the two-blade NACA propellers. M_t = 0.45.

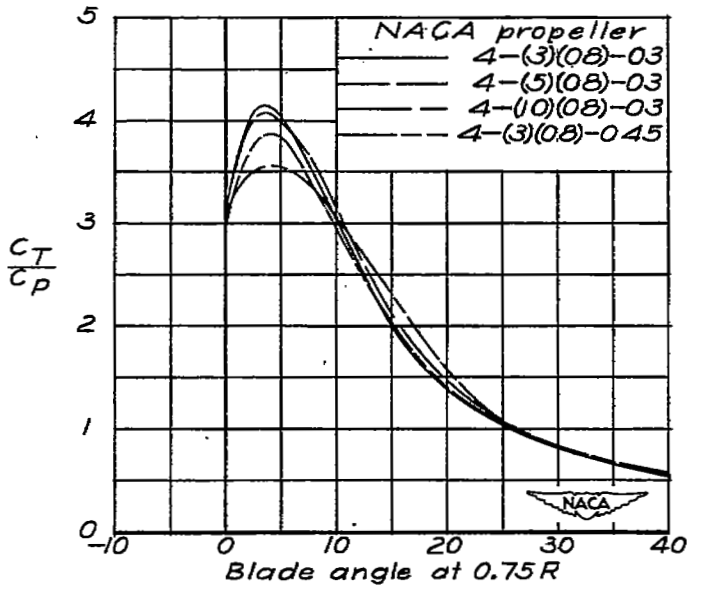

Figure 18.- Comparison of static characteristics of the two-blade NACA propellers. M_t = 0.45.

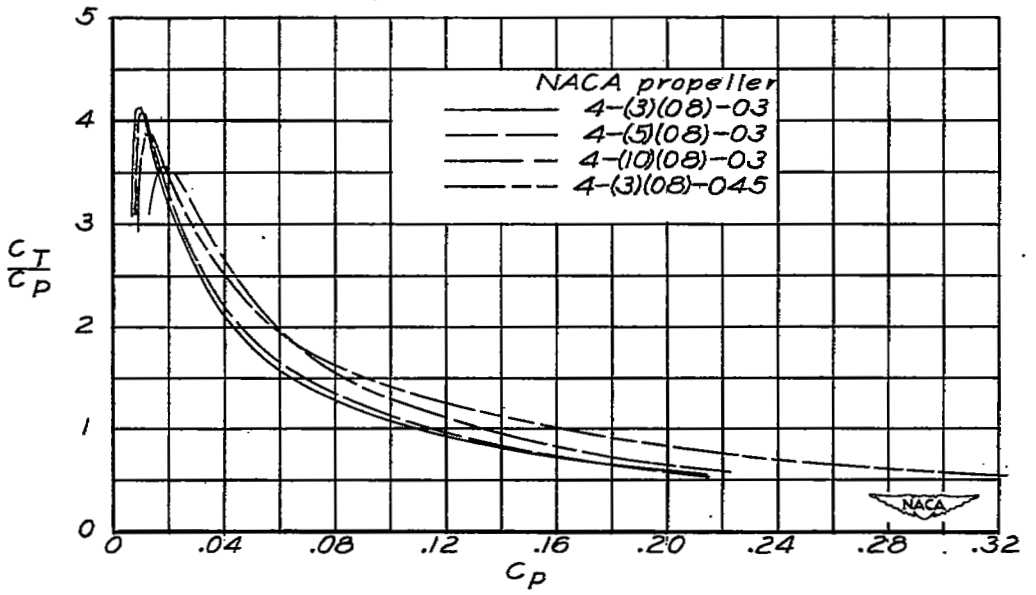

Figure 19.- Comparison of static characteristics at constant power coefficient of the two-blade NACA propellers. M_t = 0.45.

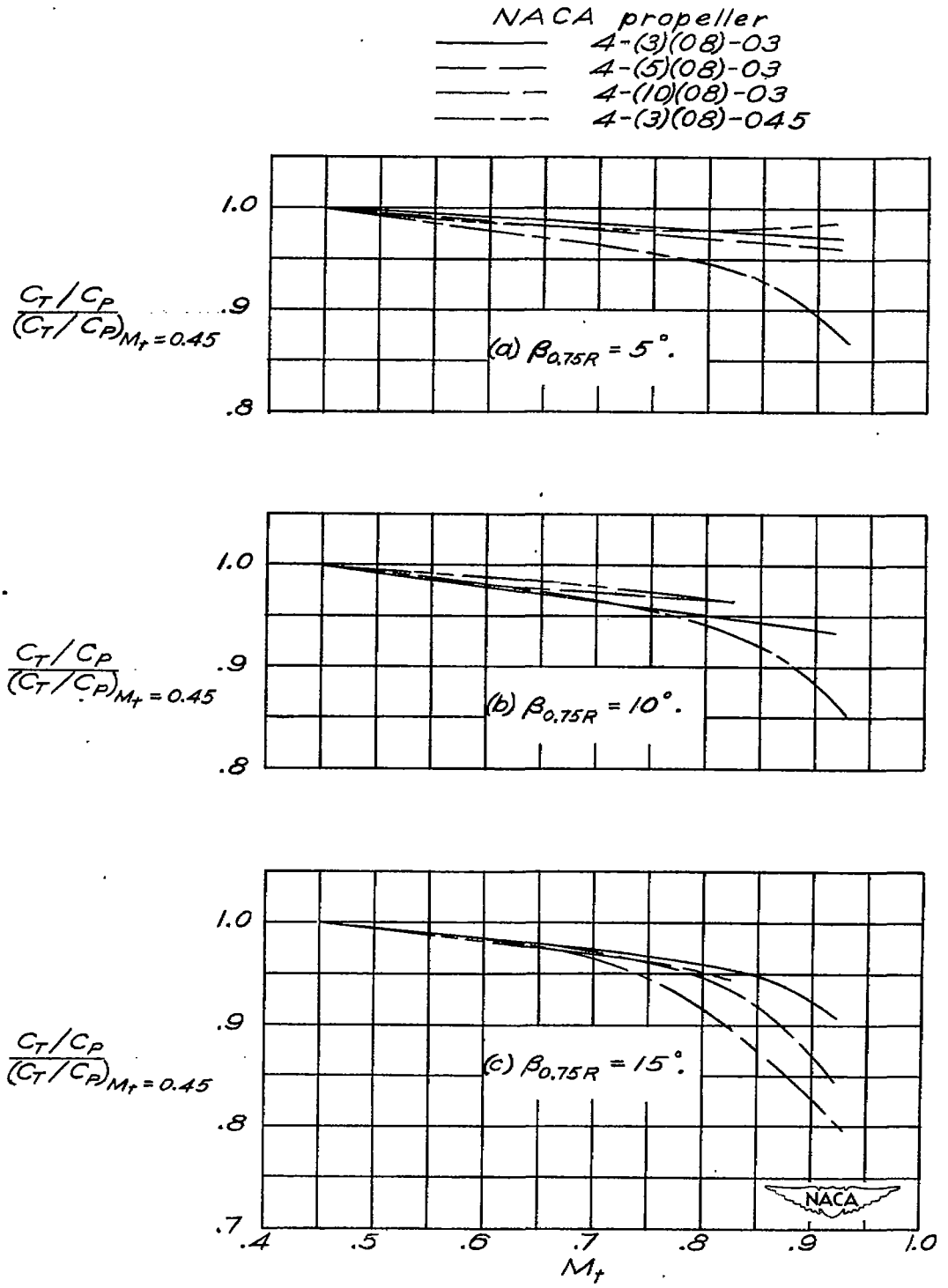

Figure 20.- Effect of tip speed. Two-blade propellers.

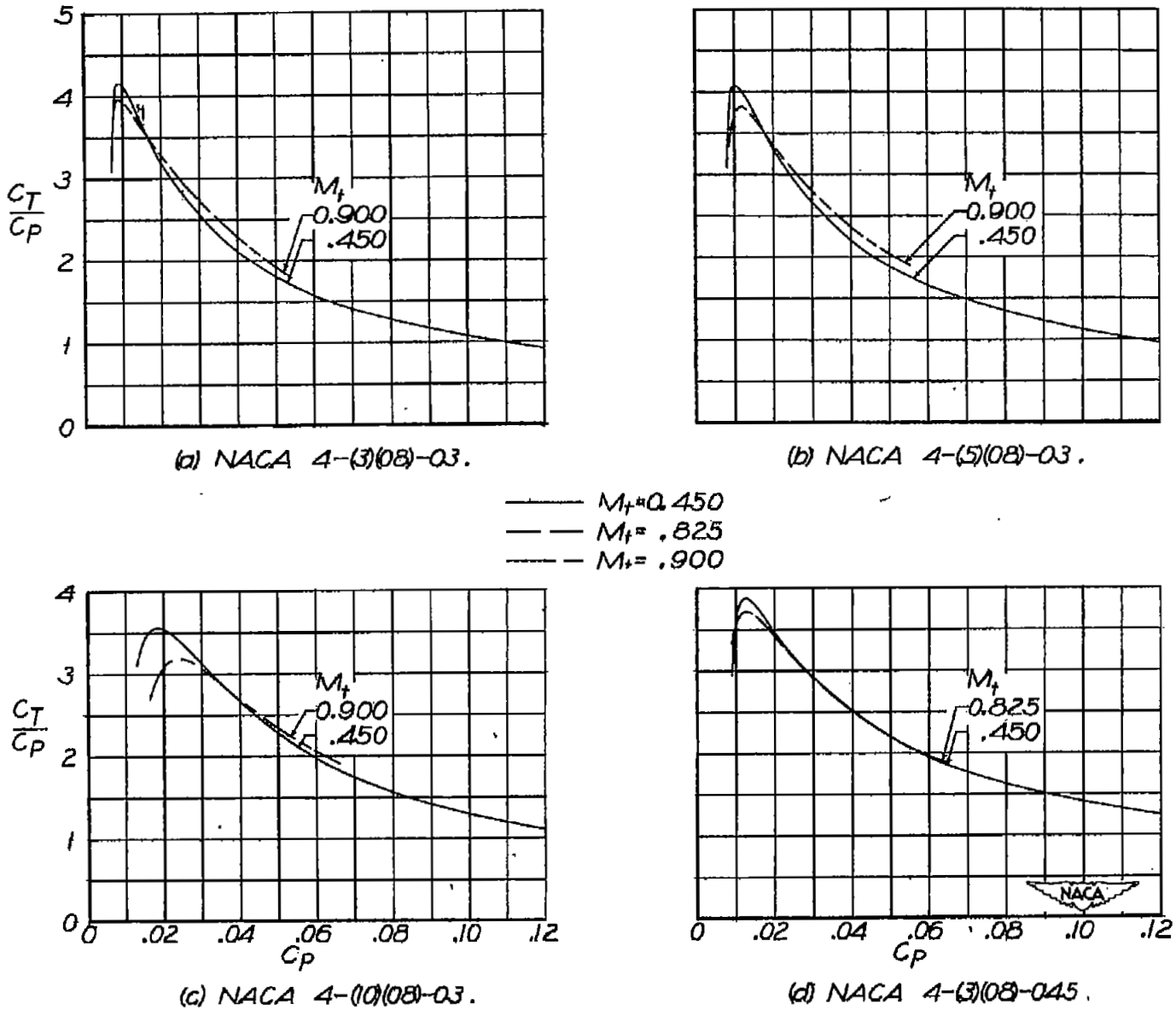

Figure 21.- Effect of tip speed. Two-blade propellers.

UNCLASSIFIED